HHS Public Access

Author manuscript

Vis Neurosci. Author manuscript; available in PMC 2015 December 02.

Published in final edited form as:

Vis Neurosci. 2015 January ; 32: E026. doi:10.1017/S0952523815000218.

Co-localization of glutamic acid decarboxylase and vesicular GABA transporter in cytochrome oxidase patches of macaque striate cortex

DANIEL L. ADAMS[1,2], **JOHN R. ECONOMIDES**[1], and **JONATHAN C. HORTON**[1]

[1]Beckman Vision Center, University of California, San Francisco, California 94143

[2]Center for Mind/Brain Sciences, The University of Trento, Trento, Italy

Abstract

The patches in primary visual cortex constitute hot spots of metabolic activity, manifested by enhanced levels of cytochrome oxidase (CO) activity. They are also labeled preferentially by immunostaining for glutamic acid decarboxylase (GAD), γ-aminobutyric acid (GABA), and parvalbumin. However, calbindin shows stronger immunoreactivity outside patches. In light of this discrepancy, the distribution of the vesicular GABA transporter (VGAT) was examined in striate cortex of two normal macaques. VGAT immunoreactivity was strongest in layers 4B, 4Cα, and 5. In tangential sections, the distribution of CO, GAD, and VGAT was compared in layer 2/3. There was a close match between all three labels. This finding indicates that GABA synthesis is enriched in patches, and that inhibitory synapses are more active in patches than interpatches.

Keywords

Cytochrome oxidase; Inhibition; Ocular dominance column; GABA; Macaque; Primary visual cortex; V1; Blob

Introduction

Tissue histochemistry for the mitochondrial enzyme, cytochrome oxidase (CO), reveals a curious array of vertical columns in the primary visual cortex (striate cortex, V1). These zones of enhanced metabolic activity, known as “patches” or “blobs”, are most striking in layers 2/3 (Hendrickson et al., 1981; Horton & Hubel, 1981). Their function remains unclear. In human and macaque, they are arranged in rows that are aligned with ocular dominance columns in layer 4 (Horton, 1984). However, in squirrel monkey, bushbaby, and owl monkey, the ocular dominance columns bear no relationship to CO patches (Xu et al., 2005; Adams & Horton, 2006; Kaskan et al., 2007). In the upper layers, CO patches receive a direct projection from koniocellular neurons in the lateral geniculate nucleus (Livingstone & Hubel, 1982; Fitzpatrick et al., 1983; Horton, 1984; Hendry & Yoshioka, 1994; Ding & Casagrande, 1997). This input may account for why patches stain more darkly for CO. The

Address correspondence to: Jonathan C. Horton MD, PhD, Beckman Vision Center, University of California, San Francisco, 10 Koret Way, San Francisco, CA 94143-0730. hortonj@vision.ucsf.edu.

layers of the cortex that receive a direct geniculate projection—2/3, 4C, 4A, and 6—exhibit the highest levels of CO activity in striate cortex.

Soon after the CO patches were discovered, they were shown in layer 2/3 to coincide with the pattern seen by immunocytochemical staining for glutamic acid decarboxylase (GAD) (Hendrickson et al., 1981). This enzyme is concentrated in the somata of inhibitory neurons, where γ-aminobutyric acid (GABA) is synthetized. After synthesis, GABA is packaged into synaptic vesicles by a vesicular GABA transporter (VGAT) (McIntire et al., 1997). VGAT is localized preferentially to nerve terminals, and its staining pattern is thought to correspond most closely to the actual distribution of inhibitory synapses in brain tissue (Conti et al., 2004). It is conceivable that GABAergic neurons are located preferentially in CO patches, but the bulk of their axonal projections terminates outside patches. In that case, one might expect to find a discrepancy between the patterns of GAD and VGAT labeling. To investigate this possibility, we compared the density of GAD and VGAT labeling with the layout of CO patches in layer 2/3 of macaque striate cortex.

Materials and methods

Experiments were conducted in two Rhesus monkeys obtained from the California National Primate Research Center, Davis, CA. The animals were mature females being used by other laboratories for experiments unrelated to neuroscience. The brains were donated for our research. Procedures were approved by the Institutional Animal Care and Use Committee at the University of California, Davis.

Each animal was killed with an intravenous injection of pentobarbital (150 mg/kg). No perfusion was performed. The brain was removed and placed into 2% paraformaldehyde in 0.1 M phosphate buffer solution (PBS), pH 7.4, at 4°C. The next day each occipital operculum was removed and immersed in 2% paraformaldehyde in 0.1 M PBS with 30% sucrose for 2 days at room temperature. A glass slide was placed against the pial surface with a 50 g weight on top to flatten the block. Tangential sections were cut at 30 μm on a freezing microtome. Every third section was mounted on a slide and dried. It was subsequently reacted for CO activity (Wong-Riley, 1979). The other two sections were collected in 10 mM phosphate buffered saline and processed free-floating for either GAD or VGAT immunocytochemistry.

GAD immunocytochemistry was performed using standard methods (Hendrickson et al., 1981; Hendry, 1991; Weltzien et al., 2014). In brief, sections were preincubated in 10 mM phosphate buffered saline containing 0.3% Triton-X and 10% normal horse serum for 4 h. Next, they were incubated in 10 mM phosphate buffered saline with 1% normal horse serum containing a mouse monoclonal antibody specific for primate GAD 65/67 (San Cruz Biotechnology sc-365180) at a dilution of 1:500 for 2 days. After exposure to a secondary antibody for 4 h, the sections were processed using the avidin-biotin-peroxidase technique (Elite ABC kit, Vector Laboratories). Peroxidase activity was revealed by reacting the sections in 3,3′-diaminobenzidine with 0.1% H_2O_2. Sections were mounted onto glass slides, air dried, and coverslipped with Permount.

VGAT immunocytochemistry was carried out in similar fashion (Chaudhry et al., 1998). A mouse monoclonal antibody to VGAT (Synaptic Systems, 031011) was used at a dilution of 1:1000.

Results

The densest CO activity was present in layers 4A and 4C, followed by layers 2/3 and 6 (Fig. 1). VGAT immunostaining was richest in the upper portion of layer 4 and layer 5, with an intermediate level in layer 2/3. Interestingly, VGAT immunostaining at the base of layer 4C was relatively weak, where CO activity was maximal.

A tangential section through layer 2/3 showed a typical array of CO patches (Fig. 2). Although the ocular dominance columns were not labeled, it was obvious that the patches were organized into parallel rows, which approached the V1/V2 border at right angles. An adjacent section processed for GAD showed a similar array of patches, as expected (Hendrickson et al., 1981). There was some blotchy unevenness to the overall intensity of labeling, which often occurs when performing immunocytochemistry in large free-floating tissue sections. The reason is unclear. The next section, processed for VGAT, also showed an array of patches throughout layer 2/3. The labeling was also uneven, but nevertheless, in some regions a pattern of patches was quite clear.

At higher magnification, comparison of the CO patches with the pattern of GAD immunolabeling showed a match (Fig. 3). There was also a close correspondence between the pattern formed by the CO patches and patches of dark VGAT immunolabeling.

The distribution of CO, GAD, and VGAT was examined in a second monkey. This animal also showed patches of GAD and VGAT immunolabeling, which coincided with the location of CO patches in the upper layers.

Discussion

Compared to interpatches, the patches in striate cortex are enriched not only in CO activity but also in lactate dehydrogenase, succinate dehydrogenase, β-nicotinamide adenine dinucleotide, acetyl-cholinesterase, myelin, nitric oxide synthase, tachykinin, NMDA receptors, AMPA receptors, Na–K ATPase, glutamate, CAT-301, and microtubule-associated protein (for review, see Horton & Adams, 2005). It might have seemed a foregone conclusion that the patches would also show strong immunoreactivity for VGAT, given that they have increased levels of so many other different enzymes, neurotransmitters, receptors, and structural proteins. Inexplicably, however, CO patches contain less zinc, calcineurin, and neurofilament protein than interpatches (Goto & Singer, 1994; Duffy & Livingstone, 2003; Dyck et al., 2003). Therefore, not every substance exhibits a greater content within CO patches.

Our results confirmed that CO patches have increased GAD levels (Hendrickson et al., 1981; Fitzpatrick et al., 1987). We used an antibody that binds to both GAD65 and GAD67. Most neurons contain both isoforms, with the latter being predominant in striate cortex (Hendrickson et al., 1994). The richer GAD labeling in patches probably reflects a higher

content of the synthetic enzyme in both cell bodies and nerve terminals. Fitzpatrick et al. (1987) have shown that the concentration of GAD-positive neurons is no higher in patches than in interpatches. It is possible, however, that cell bodies situated in patches contain higher levels of GAD than those in interpatches. Inhibitory nerve terminals in patches may also be larger, more plentiful, or contain more GAD than those in interpatches.

Immunostaining for GABA and for $GABA_A$ receptors shows a pattern of labeling that matches the CO patches (Hendry & Carder, 1992; Hendry et al., 1994). The same is true for parvalbumin, a calcium-binding protein associated with GABAergic interneurons. However, calbindin, another calcium-binding protein associated with GABAergic interneurons, is exceptional. It shows reduced immunoreactivity in layer 2/3 in zones that correspond to CO patches (Celio et al., 1986). Compared with parvalbumin, calbindin is relatively less abundant in layers that receive a direct projection from the lateral geniculate nucleus. The fact that patches receive a direct geniculate input may explain why their calbindin content is lower.

Cortical layers that receive direct input from the lateral geniculate nucleus exhibit increased CO activity (Horton, 1984). This increased CO content is correlated with a higher neuronal firing rate (DeYoe et al., 1995). This relationship also holds true in the vertical domain: cells in CO patches have a greater overall firing rate than cells in interpatches (Economides et al., 2011). To explain this finding, one might propose the following idea. Inhibitory neurons located in patches are more active than those in interpatches, as reflected by their higher levels of GAD and GABA. Suppose also that the inhibitory neurons in patches make axonal projections predominately outside patches. This would cause enhanced suppression of cells in interpatches, accounting for their lower firing rate. This hypothesis is ruled out by our finding that VGAT immunoreactivity is stronger in CO patches than interpatches. In fact, both excitatory synapses and inhibitory synapses are more active in patches compared to interpatches (Wong-Riley, 1994; Nie & Wong-Riley, 1996).

Recently, progress has been made in classifying the diverse populations of GABAergic interneurons in the cortex (DeFelipe et al., 2013). Unfortunately, we could not distinguish reliably the morphology of different GABAergic interneurons in tissue sections processed for GAD immunocytochemistry. In any case, so far, no class of morphologically distinct cortical neurons has been found to be located preferentially within CO patches in layer 2/3 (Hübener & Bolz, 1992). It is surprising that patches have unique inputs and outputs but no predilection for a particular cortical cell type.

In striate cortex, the laminar distribution of CO, GAD, GABA, and the subunits of the $GABA_A$ receptor are similar (Fitzpatrick et al., 1987; Hendry & Carder, 1992; Hendry et al., 1994). Their activity is most robust in the layers (2/3, 4A, 4C, 6) that receive direct input from the lateral geniculate nucleus. Surprisingly, the laminar distribution of VGAT was quite different (Fig. 1). This finding was not expected and remains to be correlated with the organization of the interlaminar projections of inhibitory cells in striate cortex.

Acknowledgments

Technical support was provided by Valerie L. Wu. We thank Stewart Hendry and Robert Edwards for advice regarding GAD and VGAT immunohistochemistry, respectively. This work was supported by grants EY10217 (J.C.H.), EY02162 (Beckman Vision Center) from the National Eye Institute and a Physician Scientist award from Research to Prevent Blindness. The California National Primate Research Center is supported by NIH Base Grant RR00169.

References

Adams DL, Horton JC. Monocular cells without ocular dominance columns. Journal of Neurophysiology. 2006; 96:2253–2264. [PubMed: 16855115]

Celio MR, Scharer L, Morrison JH, Norman AW, Bloom FE. Calbindin immunoreactivity alternates with cytochrome c-oxidase-rich zones in some layers of the primate visual cortex. Nature. 1986; 323:715–717. [PubMed: 3022149]

Chaudhry FA, Reimer RJ, Bellocchio EE, Danbolt NC, Osen KK, Edwards RH, Storm-Mathisen J. The vesicular GABA transporter, VGAT, localizes to synaptic vesicles in sets of glycinergic as well as GABAergic neurons. The Journal of Neuroscience. 1998; 18:9733–9750. [PubMed: 9822734]

Conti F, Minelli A, Melone M. GABA transporters in the mammalian cerebral cortex: Localization, development and pathological implications. Brain Research. Brain Research Reviews. 2004; 45:196–212. [PubMed: 15210304]

DeFelipe J, Lopez-Cruz PL, Benavides-Piccione R, Bielza C, Larranaga P, Anderson S, Burkhalter A, Cauli B, Fairen A, Feldmeyer D, Fishell G, Fitzpatrick D, Freund TF, Gonzalez-Burgos G, Hestrin S, Hill S, Hof PR, Huang J, Jones EG, Kawaguchi Y, Kisvarday Z, Kubota Y, Lewis DA, Marin O, Markram H, McBain CJ, Meyer HS, Monyer H, Nelson SB, Rockland K, Rossier J, Rubenstein JL, Rudy B, Scanziani M, Shepherd GM, Sherwood CC, Staiger JF, Tamas G, Thomson A, Wang Y, Yuste R, Ascoli GA. New insights into the classification and nomenclature of cortical GABAergic interneurons. Nature Reviews. Neuroscience. 2013; 14:202–216.

DeYoe EA, Trusk TC, Wong-Riley MT. Activity correlates of cytochrome oxidase-defined compartments in granular and supra-granular layers of primary visual cortex of the macaque monkey. Visual Neuroscience. 1995; 12:629–639. [PubMed: 8527365]

Ding Y, Casagrande VA. The distribution and morphology of LGN K pathway axons within the layers and CO blobs of owl monkey V1. Visual Neuroscience. 1997; 14:691–704. [PubMed: 9278998]

Duffy KR, Livingstone MS. Distribution of non-phosphorylated neurofilament in squirrel monkey V1 is complementary to the pattern of cytochrome-oxidase blobs. Cerebral Cortex. 2003; 13:722–727. [PubMed: 12816887]

Dyck RH, Chaudhuri A, Cynader MS. Experience-dependent regulation of the zincergic innervation of visual cortex in adult monkeys. Cerebral Cortex. 2003; 13:1094–1109. [PubMed: 12967926]

Economides JR, Sincich LC, Adams DL, Horton JC. Orientation tuning of cytochrome oxidase patches in macaque primary visual cortex. Nature Neuroscience. 2011; 14:1574–1580. [PubMed: 22057193]

Fitzpatrick D, Itoh K, Diamond IT. The laminar organization of the lateral geniculate body and the striate cortex in the squirrel monkey (*Saimiri sciureus*). The Journal of Neuroscience. 1983; 3:673–702. [PubMed: 6187901]

Fitzpatrick D, Lund JS, Schmechel DE, Towles AC. Distribution of GABAergic neurons and axon terminals in the macaque striate cortex. The Journal of Comparative Neurology. 1987; 264:73–91. [PubMed: 3680625]

Goto S, Singer W. Laminar and columnar organization of immunoreactivity for calcineurin, a calcium- and calmodulin-regulated protein phosphatase, in monkey striate cortex. Cerebral Cortex. 1994; 4:636–645. [PubMed: 7703689]

Hendrickson AE, Hunt SP, Wu JY. Immunocytochemical localization of glutamic acid decarboxylase in monkey striate cortex. Nature. 1981; 292:605–607. [PubMed: 6265804]

Hendrickson AE, Tillakaratne NJ, Mehra RD, Esclapez M, Erickson A, Vician L, Tobin AJ. Differential localization of two glutamic acid decarboxylases (GAD65 and GAD67) in adult

monkey visual cortex. The Journal of Comparative Neurology. 1994; 343:566–581. [PubMed: 8034788]

Hendry S, Carder RK. Organization and plasticity of GABA neurons and receptors in monkey visual cortex. Progress in Brain Research. 1992; 90:477–502. [PubMed: 1321463]

Hendry SH. Delayed reduction in GABA and GAD immunoreactivity of neurons in the adult monkey dorsal lateral geniculate nucleus following monocular deprivation or enucleation. Experimental Brain Research. 1991; 86:47–59. [PubMed: 1756798]

Hendry SH, Huntsman MM, Viñuela A, Möhler H, de Blas AL, Jones EG. GABAA receptor subunit immunoreactivity in primate visual cortex: Distribution in macaques and humans and regulation by visual input in adulthood. The Journal of Neuroscience. 1994; 14:2383–2401. [PubMed: 8158275]

Hendry SH, Yoshioka T. A neurochemically distinct third channel in the macaque dorsal lateral geniculate nucleus. Science. 1994; 264:575–577. [PubMed: 8160015]

Horton JC. Cytochrome oxidase patches: A new cytoarchitectonic feature of monkey visual cortex. Philosophical Transactions of the Royal Society of London. Series B, Biological Sciences. 1984; 304:199–253. [PubMed: 6142484]

Horton JC, Adams DL. The cortical column: A structure without a function. Philosophical Transactions of the Royal Society of London. Series B, Biological Sciences. 2005; 360:837–862. [PubMed: 15937015]

Horton JC, Hubel DH. Regular patchy distribution of cytochrome oxidase staining in primary visual cortex of macaque monkey. Nature. 1981; 292:762–764. [PubMed: 6267472]

Hübener M, Bolz J. Relationships between dendritic morphology and cytochrome oxidase compartments in monkey striate cortex. The Journal of Comparative Neurology. 1992; 324:67–80. [PubMed: 1328331]

Kaskan PM, Lu HD, Dillenburger BC, Roe AW, Kaas JH. Intrinsic-signal optical imaging reveals cryptic ocular dominance columns in primary visual cortex of New World owl monkeys. Frontiers in Neuroscience. 2007; 1:67–75. [PubMed: 18974855]

Livingstone MS, Hubel DH. Thalamic inputs to cytochrome oxidase-rich regions in monkey visual cortex. Proceedings of the National Academy of Sciences of the United States of America. 1982; 79:6098–6101. [PubMed: 6193514]

McIntire SL, Reimer RJ, Schuske K, Edwards RH, Jorgensen EM. Identification and characterization of the vesicular GABA transporter. Nature. 1997; 389:870–876. [PubMed: 9349821]

Nie F, Wong-Riley MT. Differential glutamatergic innervation in cytochrome oxidase-rich and -poor regions of the macaque striate cortex: Quantitative EM analysis of neurons and neuropil. The Journal of Comparative Neurology. 1996; 369:571–590. [PubMed: 8761929]

Weltzien F, Dimarco S, Protti DA, Daraio T, Martin PR, Grunert U. Characterization of secretagogin-immunoreactive amacrine cells in marmoset retina. The Journal of Comparative Neurology. 2014; 522:435–455. [PubMed: 23852983]

Wong-Riley MTT. Changes in the visual system of monocularly sutured or enucleated cats demonstrable with cytochrome oxidase histochemistry. Brain Research. 1979; 171:11–28. [PubMed: 223730]

Wong-Riley, MTT. Primate visual cortex: Dynamic metabolic organization and plasticity revealed by cytochrome oxidase. In: Peters, A.; Rockland, KS., editors. Cerebral Cortex. New York: Plenum Press; 1994. p. 141-200.

Xu X, Bosking WH, White LE, Fitzpatrick D, Casagrande VA. Functional organization of visual cortex in the prosimian bush baby revealed by optical imaging of intrinsic signals. Journal of Neurophysiology. 2005; 94:2748–2762. [PubMed: 16000523]

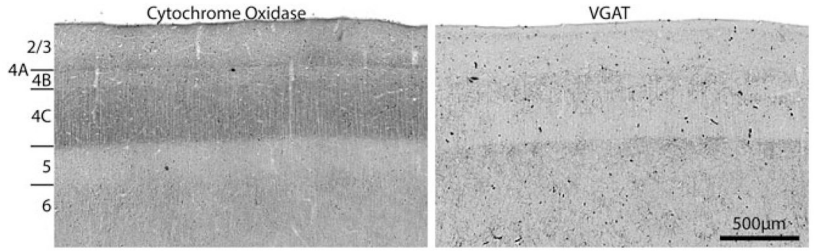

Fig. 1.

Laminar distribution of CO and VGAT in macaque striate cortex. CO is darkest in layers 4C and 4A. VGAT immunostaining is strongest in upper layer 4 and layer 5. The sharpest transition is at the layer 4C/5 border, where the labels are opposite in distribution.

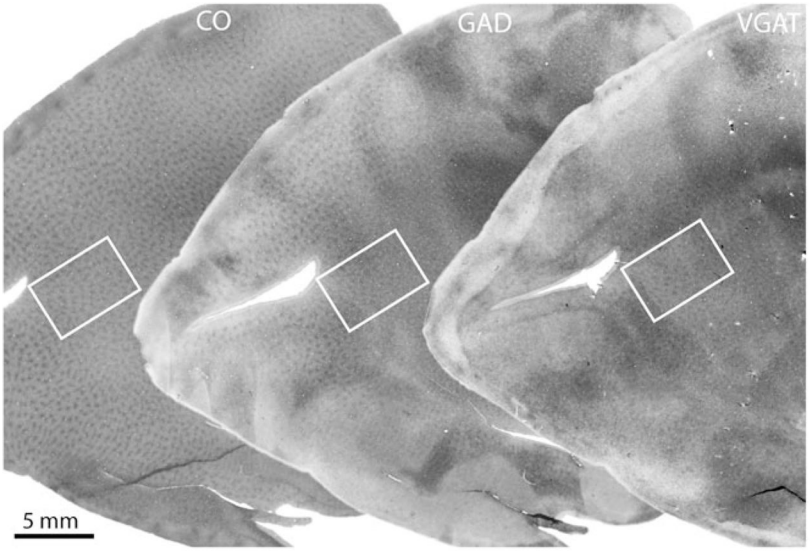

Fig. 2.

Comparison of CO, GAD, and VGAT in macaque striate cortex. The far left section shows the array of CO patches in layer 3. An adjacent section, pictured in the middle, shows a similar appearance of GAD patches. The next section, at the right, shows patches of VGAT. Regions enclosed by the white rectangles are shown in Fig. 3.

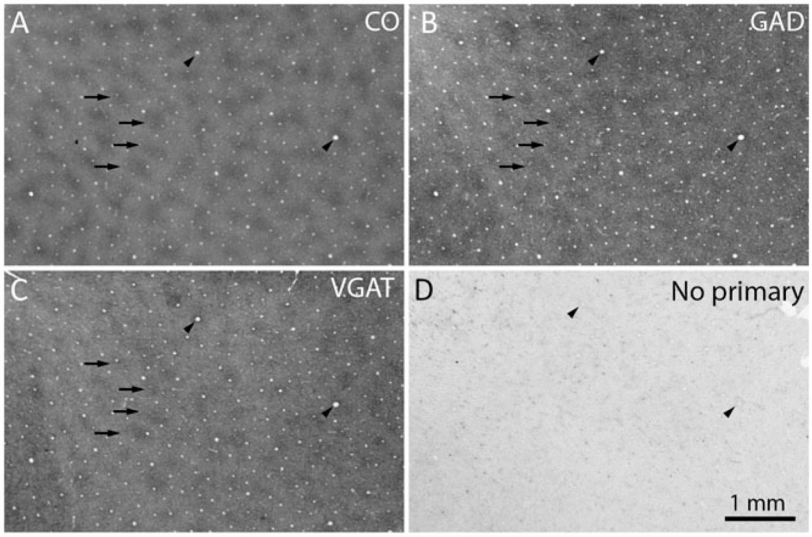

Fig. 3.

GAD and VGAT are localized preferentially in CO patches. (**a**) CO patches, with 4 examples highlighted by arrows. The arrowheads mark prominent blood vessels, which allow precise alignment of adjacent sections. (**b**) GAD patches, which match the CO patches (arrows). (**c**) VGAT patches, which match the CO and GAD patches (arrows). (**d**) Control section omitting the primary antibody shows only light background labeling from endogenous peroxidase activity in red blood cells.